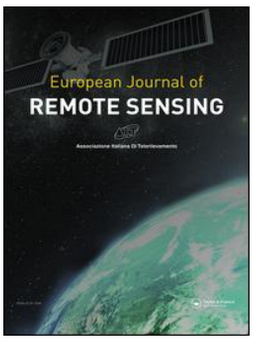

European Journal of Remote Sensing

ISSN: (Print) 2279-7254 (Online) Journal homepage: http://www.tandfonline.com/loi/tejr20

Estimation of canopy cover in dense mixed-species forests using airborne lidar data

Tauri Arumäe & Mait Lang

To cite this article: Tauri Arumäe & Mait Lang (2018) Estimation of canopy cover in dense mixed-species forests using airborne lidar data, European Journal of Remote Sensing, 51:1, 132-141, DOI: 10.1080/22797254.2017.1411169

To link to this article: https://doi.org/10.1080/22797254.2017.1411169

EUROPEAN JOURNAL OF REMOTE SENSING, 2017
VOL. 51, NO. 1, 132–141
https://doi.org/10.1080/22797254.2017.1411169

Taylor & Francis
Taylor & Francis Group

Estimation of canopy cover in dense mixed-species forests using airborne lidar data

Tauri Arumäe[a,b] and Mait Lang[a,c]

[a]Institute of Forestry and Rural Engineering, Estonian University of Life Sciences, Tartu, Estonia; [b]Forest survey management division, State Forest Management Centre, Tallinn, Estonia; [c]Department of Remote Sensing, Tartu Observatory, Tõravere, Tartumaa, Estonia

ABSTRACT

Airborne laser scanning (ALS) data and digital hemispherical photos (DHP) from 93 sample plots in Laeva test site, Estonia, were used to study effects of phenology and scan angle on the ALS-based canopy cover (CC_{ALS}) estimates. The relative share of first returns ($P_{1/A}$) for 6185 forest stands was analysed. The CC_{ALS} was calculated using different height thresholds and echoes, and was compared with the CC estimates based on DHP (CC_{DHP}) and crown model (CC_{RCrown}). The first of many echoes-based canopy cover estimate ($CC_{ALS,1.3\_1}$) saturated at values greater than 80%. The strongest correlation of CC_{DHP} was found with $CC_{ALS,1.3\_A}$ using all echoes and a 1.3 m height break (R^2 = 0.81, $RMSE$ = 11.8%). Correcting the estimate for view nadir angle did not improve the correlation of $CC_{ALS,1.3\_A}$ with CC_{DHP}. The CC_{RCrown} had a weak correlation (R^2 < 0.25) with CC_{ALS} and with CC_{DHP}. The $P_{1/A}$ was not influenced by tree species composition, but by phenology, stand relative density and forest height; however, CC_{ALS} was not dependent on stand height. Foliage phenology had a substantial effect on CC_{ALS} and CC_{DHP}. In dense mixed-species forests, we recommend to use all returns for canopy cover estimation.

ARTICLE HISTORY
Received 9 February 2017
Revised 30 June 2017
Accepted 25 November 2017

KEYWORDS
Airborne lidar data; canopy cover; tree crown models; live crown base height; phenology

Introduction

Airborne laser scanning (ALS) has become a widely used remote sensing method for assessing forest structure variables in operational forestry (Andersen, McGaughey & Reutebuch, 2005). The main applications of ALS are forest height map construction (Arumäe & Lang, 2016a; Næsset, 1997a), wood volume and biomass estimation (Bouvier, Durrieu, Fournier, & Renaud, 2015; Ferraz et al., 2016; Guerra-Hernández et al., 2016; Næsset, 1997b; Patenaude et al., 2004, Popescu, Zhao, Neuenschwander, & Lin, 2011), carbon stock monitoring (Bright, Hicke, & Hudak, 2012) and biodiversity mapping (Müller & Vierling, 2014; Smith, Anderson, & Fladeland, 2008). Vertical canopy cover (CC) is the key factor for most of these estimates and when combined with other forest structure parameters it is used for leaf-area index (LAI) mapping (Korhonen & Morsdorf, 2014; Solberg et al., 2009) or could be used for planning of thinnings in forest management (Vastaranta et al., 2011). Forest canopy structure is additionally described with mean tree height (H), crown length and the ratio of crown length to H, crown cover, effective CC and angular canopy closure. Distinguishing between different CC estimates is essential for forest structure studies (Jennings, Brown, & Sheil, 1999; Korhonen, Korpela, Heiskanen, & Maltamo, 2011). The CC, as defined by Jennings et al. (1999) and as used in this study, is the share of ground covered by the vertical projection of the canopy and is commonly expressed as a percentage. The simplest method for measuring vertical CC is using the Cajanus tube (Korhonen, Korhonen, Rautiainen, & Stenberg, 2006; Rautiainen, Stenberg, & Nilson, 2005). Canopy closure, on the other hand, is defined as the proportion of the sky hemisphere obscured by the vegetation canopy when viewed from a single point (Jennings et al., 1999). Canopy closure can be estimated from digital hemispherical photos (DHP) or measured using the LAI-2000 plant canopy analyser (Jonckheere, Nackaerts, Muys, & Coppin, 2005).

The CC and crown cover (ratio of the total area of crown vertical projections divided by the sampling area) are also estimated using crown radius models and stand density (Spurr, 1948). Tree crown radius is commonly estimated using stem diameter at breast height (Davies & Pommerening, 2008; Spurr, 1948) and can be used for tree competition assessment (Purves, Lichstein, & Pacala, 2007). The relationship between stem diameter at breast height, tree crown radius and CC can be used to estimate the mean tree size from ALS data (Ferraz, Saatchi, Mallet, & Meyer, 2016). However, crown radius models may yield different crown cover estimates, depending on the definition of tree crowns, tree species and age (Kandare, Ørka, Dalponte, Næsset, & Gobakken, 2017).

CONTACT Tauri Arumäe tauri.arumae@rmk.ee Institute of Forestry and Rural Engineering, Estonian University of Life Sciences, Kreutzwaldi 5, Tartu 51014, Estonia

Commonly, tree crowns are modelled as solid geometrical shapes – a cone, ellipsoid (Kuusk & Nilson, 2000) or convex irregular polygon (Mongus & Žalik, 2015). If gaps in the tree crown are accounted, then the result is an effective CC estimate (Duncanson, Cook, Hurtt, & Dubayah, 2014).

A DHP records all the radiation penetrating through tree crown or plant canopy, taking into account all the gaps inside the tree crowns, and the share of sky pixels in the total number of pixels is the effective canopy closure. For the conversion of canopy closure into CC, the view zenith angle should not exceed 20° (Korhonen, Korpela, Heiskanen & Maltamo, 2011) and the estimates should be corrected for within-crown gap fraction (Nilson & Kuusk, 2004). The sources of uncertainties in the ALS data-based estimates of CC (CC_{ALS}) are related to the scanning setup where the view nadir angle (VNA) is usually in the range of $0° \leq VNA \leq 30°$ and the angular dependence of the observations is characteristic of canopy closure. There are no clear rules of how to account for within-crown gaps. The pulse footprint of the scanners is commonly larger than gaps inside crowns. For example, Leica ALS50-II at a 2400-m flight altitude and beam divergence of 0.22 mrad (Leica, 2007) has a pulse footprint of about 50 cm in diameter. The canopy itself is also semi-transparent on near-infrared (NIR) wavelengths used in most of the topographic mapping oriented ALS devices, so defining crown gaps is problematic. A laser scanner can also retrieve echoes from overlapping crowns, which would allow estimating crown cover, when the overlapping areas of the crowns are taken into account separately.

The most common method for the CC_{ALS} estimation is using a height break or threshold and calculating the share of the first and first of many echoes above the height break in the total number of echoes (Korhonen, Korpela, Heiskanen & Maltamo, 2011). The threshold is commonly set at a few metres above the ground corresponding to the live crown base height (Smith et al., 2009). However, it is found that the CC_{ALS} estimate based on the first and first of many echoes using the, e.g. Leica ALS50-II scanner will result in the CC_{ALS} estimate saturation, especially in dense deciduous forests (Lang, 2010; Lang, Arumäe, & Anniste, 2012). The CC_{ALS} is influenced also by scanning parameters (Keränen, Maltamo, & Packalen, 2016) and the ratio of the first echo count to all echoes ($P_{1/A}$) which characterizes pulse splitting and is affected by phenology stages, especially for deciduous forests (Wasser, Day, Chasmer, & Taylor, 2013). In NIR spectral region, broadleaved deciduous tree species have a higher reflectance than needle leaf species (Kuusk, Lang, & Kuusk, 2013) which can also influence the $P_{1/A}$. As a result, CC is at best estimated from ALS data with a root mean square error of 10% (Ferraz et al., 2015). Similar results are shown for canopy closure estimates (Moeser, Roubinek, Schleppi, Morsdorf, & Jonas, 2014). In practical applications where CC_{ALS} or its analogues are used for ALS-based wood volume models (Arumäe & Lang, 2016b; Bouvier et al., 2015) an error of 10% in CC_{ALS} causes about a 15% difference in predicted wood volume.

The aim of this study was to test different CC_{ALS} estimation methods in dense deciduous broadleaf-dominated hemi-boreal forests stands. The ALS data were from two phenological phases – before bud swelling with leaves off (bBS) and after the final leaf unfolding stage (aFLU) with leaves fully developed. CC estimates from DHP (CC_{DHP}) were chosen as the reference for other methods. Additional tests were carried out using CC estimates based on tree position data and the crown radius model (CC_{RCrown}). The influence of scan angle, $P_{1/A}$ and plot location on the CC_{ALS} estimates was investigated.

Materials and methods

Study site

The 15 × 15 km test site is located in south-eastern Estonia, near Laeva (Lang, Arumäe, Lükk, & Sims, 2014). The terrain is rather flat. Half of the area is covered by forests. The forests are of mixed species and multi-layer structure is common, with a dense understory layer of *Padus avium* Mill. and *Corylus avellana* L. Dominant tree species are silver birch (*Betula pendula* Roth), Norway spruce (*Picea abies* L.), trembling aspen (*Populus tremula* L.), black alder (*Alnus glutinosa* L.) and Norway spruce in the lower layer. The most common site types are the *Aegopodium* and *Filipendula* (Lõhmus, 2004) and based on FAO-UNESCO, the soil types are mainly fertile *Calci Eutric Gleysols* and *Eutri Histic Gleysols*. The forest height can reach up to 37 m (typical height in mature forests is 25–30 m) and the basal area is up to 40 m^2/ha according to forest inventory (FI) data.

The first dataset in the tests was FI data for 6185 stands. The FI data were used for studying the influence of deciduous species fraction on $P_{1/A}$. The majority of the stands were inventoried in 2013. The average stand size was 2.0 ha and dominating tree species are silver birch and trembling aspen with a common second layer of Norway spruces. The second dataset was based on 93 sample plots extracted from the Estonian Network of Forest Research (ENFR) database (Kiviste et al., 2015). According to Kiviste et al. (2015) all the trees on these plots were calipered, tree positions were mapped and model trees were selected for crown base height and height measurements. The rest of the tree heights were estimated using diameter-height

models based on sample tree measurements. Dominating tree species in the ENFR plots are silver birch and trembling aspen, with an average age of 59 years for silver birch and 65 years for trembling aspen. The average height of the forests was 23 m and basal area average was 25 m^2/ha. The average relative density (also known as stand stocking index) was 81%.

ALS data

The ALS data were collected in spring (06 May 2013) and summer (13 July 2013) by the Estonian Land Board using the scanner Leica ALS50-II. The ALS point density for bBS was 0.5 points/m^2, the flight altitude was 2400 m and ALS pulse footprint diameter on the ground was 50 cm. Point density for aFLU dataset was 2 points/m^2, flight altitude 1800 m and pulse footprint diameter on the ground was 40 cm in diameter. The bBS and aFLU datasets were combined in one analysis to increase the range of CC_{ALS} and to use the bBS data as a substitute for possible defoliation effects. The VNA did not exceed 28°. The ALS data were processed using FUSION/LDV freeware (McGaughey, 2014).

The CC_{ALS} was calculated using different height breaks (z) with a 1-m step starting from 1.3 m and ending at the live crown base height (H_{LCB}) to reduce the forest understory vegetation influence. The CC_{ALS} was calculated as follows:

$$CC_{ALS,z\_E} = \frac{100 \cdot P_E(h_p > z)}{P_E} \quad (1)$$

where

P – the number of echoes,
h_p – the pulse return height from the ground,
E – selection of the first or first of many ("1") or all ("A") echoes.

The ALS-based live crown base height (H_{LCB_ALS}) was estimated with the model (2) taken from Arumäe and Lang (2013), where $H_{LCB\_ALS\_0}$ is calculated using point cloud height distribution mode value (H_{Mode}) and standard deviation (H_{Stdev}) excluding the points with $h_p \leq 1.3$ m.

$$H_{LCB\_ALS\_0} = H_{Mode} - \frac{H_{Stdev}}{2} \quad (2)$$

Correlation between the measured H_{LCB} and $H_{LCB\_ALS\_0}$ was strong (R^2 = 0.79). However, $H_{LCB\_ALS\_0}$ overestimated H_{LCB} on average by 6.8 m and therefore a linear correction model (3) was applied.

$$H_{LCB\_ALS} = 0.69 \cdot H_{LCB_{ALS_0}} - 1.3 \quad (3)$$

We tested also the influence of VNA correction on CC_{ALS} depending on the selection of echoes and ALS measurement geometry. To study the CC_{ALS} dependence on scanning angle, first 38 of the ENFR plots were selected where the scan angle was large (18–28°). The sample plots occurred on the overlapping area of scan swaths and, as the result of the flight plan, they were scanned from two opposite directions (*ALS_Left; ALS_Right*). The relationship between CC_{ALS_Left} and CC_{ALS_Right} was analysed before and after the VNA correction with the model by Korhonen and Morsdorf (2014)

$$CC_{ALS} = CC_{ALS,1.3\_1} - 0.0253 \cdot \theta_{scan} \cdot F_{max}, \quad (4)$$

where

$CC_{ALS,1.3\_1}$ – the CC estimate using the first or first of many echoes,
θ_{scan} – mean scan angle (°),
F_{max} – height of the highest echo above the digital terrain model (m).

In pulse splitting analysis, both canopy and ground returns were included to test the influence of tree species on $P_{1/A}$. The impact of foliage phenology on the occurrence of returns within the canopy and the corresponding $P_{1/A}$ was analysed in the ENFR plots including only the pulse returns with $h_p > 1.3$.

Digital hemispherical photographs

The DHP measurements were carried out in the summer of 2013. On 32 out of the 93 ENFR plots, DHP measurements were carried out also in spring at the time before bud swelling. Twelve photos per plot were taken following the VALERI protocol (Validation of Land European Remote Sensing Instruments, http://www.avignon.inra.fr/valeri/). Three sampling points were marked in all four cardinal points, with a 4-m distance between each sample. For hemispherical photos, we used a Nikon D5100 with the Sigma 4.5 mm F2.8 EX DC HSM Circular Fisheye lens and a Canon EOS 5D with the Sigma 8 mm 1:3.5 EX DG Fisheye lens. The HSP software (Lang, Kodar, & Arumäe, 2013) was used for DHP processing. The CC_{DHP} for each plot was then calculated as an average of CC estimates from 12 single photos. Pixels from the view zenith angle of less than 9° were used to measure CC (corresponds roughly to the first ring of LAI-2000).

Crown radius models

Two crown radius (R_{Crown}) models were initially tested – the first model was published by Jakobsons (1970) and is based on stem diameter at breast height (d). The second R_{Crown} model (model 14 from Lang, Nilson, Kuusk, Kiviste, & Hordo, 2007) is based on tree height and d. Using the calculated R_{Crown} values, the CC (CC_{RCrown}) estimate was calculated by merging all the crown shapes. The CC_{RCrown} using

Jakobsons (1970) model was 32–42% greater compared to the CC_{RCrown} calculated using model by Lang et al. (2007). Additionally, the average CC for all 93 plots with Jakobsons' (1970) R_{Crown} model was 50% greater than with the model by Nilson, Lang, Kuusk, Anniste, and Lükk (2000) that relates $CC = 100 \cdot (0.898T + 0.044)$ where T is stand relative density. Therefore, Jakobsons' (1970) model was abandoned.

Tree crown vertical projections on the ground can be represented as concentric rings of a particular radius in the case of equal spacing of the trees. In natural stands, however, distances between trees vary and, due to the competition for light, branches grow more likely towards open space. As a result, the overlaps between tree crown projections decrease and CC increases. Since tree positions in the ENFR plots were known, a model from Lang and Kurvits (2007) was used to adjust crown projections according to the neighbours of each tree, while the area of each crown projection was fixed to that of the circle with the predicted crown radius. This model was able to draw more realistic crown shapes, and a visual comparison of the adjusted crown projections with orthophotos showed a good agreement. For each sample plot, all crown projections were then merged into one polygon using QGIS to calculate the CC_{RCrown}. After the crown shape modification, CC increased (mean CC_{CRown} by 3% and the maximum difference was 16%) compared to the circular crown projections-based CC. We assumed that this also increases the correlation with CC_{ALS}. We did not apply edge correction (see, e.g., Lilleleht, Sims, & Pommerening, 2014) and a small underestimation of CC near a sample plot border is still possible. To study the edge effect, a 2-m wide buffer was excluded from outside the sample plots. The parts of crown projections within the decreased sample plot were then extracted and CC_{RCrown} was estimated again. The CC_{RCrown} estimates were compared with the aFLU CC_{ALS}.

Manipulation of plot centre location

To estimate the stability of CC_{ALS}, the centre positions of the 93 ENFR plots were randomly dislocated for 100 times within a radius of 10 m, which corresponds roughly to the estimated maximum error in the ENFR plot coordinate measurements. The $CC_{ALS,1.3\_A}$ was calculated for each dislocated point cloud sample and variation was analysed.

Error estimates

The mean error of estimate (*MEE*) was calculated as

$$\mathrm{MEE} = \Sigma(\mathrm{X} - \mathrm{Y})/\mathrm{N} \quad (5)$$

and the root mean square error (*RMSE*) was calculated as

$$RMSE = \sqrt{\sum (X - Y)^2 / N} \quad (6)$$

where X is the argument, Y is the dependent variable and N is the number of observations.

Results

The shifting of the centre coordinate showed that the $CC_{ALS,1.3\_A}$ estimates are rather stable concerning errors in ALS point cloud sample locations. The standard error of $CC_{ALS,1.3\_A}$ for the 93 ENFR plots was 0.15% and the average interquartile range of $CC_{ALS,1.3\_A}$ was 2.2%. The largest range of $CC_{ALS,1.3\_A}$ estimates was 23%, nine sample plots had a $CC_{ALS,1.3\_A}$ range of larger than 10% and the average range of $CC_{ALS,1.3\_A}$ was 6.1%.

There was a substantial influence of phenology on the CC_{ALS} estimates. For bBS, the average $CC_{ALS,1.3\_A}$ of the ENFR plots was about 20% smaller compared to the average of aFLU conditions (Table 1).

The correlation of CC_{DHP} with the first echoes-based $CC_{ALS,1.3\_1}$ was weaker ($R^2 = 0.75$, $RMSE = 20.7\%$) than with $CC_{ALS,1.3\_A}$ ($R^2 = 0.81$, $RMSE = 11.8\%$; Figure 1, Table 1). When aFLU and bBS measurements were tested separately, the smallest *RMSE* was found for $CC_{ALS,1.3\_A}$ and CC_{DHP} of aFLU flight and the R^2 corresponded to a moderate correlation.

The change in correlation between $CC_{ALS,z}$ and CC_{DHP} when the height break was raised from $z = 1$ to $z = 5$ m was not significant. Raising the z even higher, up to 10 m, somewhat improved the predictive power of the first echoes, but the increase in R^2 was small. The $CC_{ALS,LCB}$, estimated at $z = H_{LCB\_ALS}$, had surprisingly only a weak correlation ($R^2 = 0.15$) with CC_{DHP} for aFLU dataset and no correlation for bBS measurements ($R^2 = 0$). This was most likely due to the ALS-based H_{LCB} model (2) not being able to predict the H_{LCB} for bBS dataset. The H_{Mode} for bBS data occurred near the minimum height threshold of 1.3 m following the mode value of the pulse return height distribution and the $CC_{ALS,LCB}$ was substantially overestimated. This was probably the result of a dense forest understory and second layer of spruces in many stands that caused pulse returns from below the upper tree layer and flattened the height distribution of pulse returns and changed the position of H_{Mode}. Using the measured H_{LCB}

Table 1. Relationships between CC_{DHP} and $CC_{ALS,1.3}$ depending on the phenophase and selection of pulse return.

	$CC_{1.3}$ using the first and first of many echoes (%)				$CC_{1.3}$ using all echoes (%)			
Phenophase[a]	Mean	*RMSE*	*MEE*	R^2	Mean	*RMSE*	*MEE*	R^2
bBS	74.0	34.8	−31.7	0.64	59.7	19.3	−17.3	0.62
aFLU	93.9	14.0	−11.9	0.32	83.5	7.4	−1.5	0.37
Combined	-	20.7	−17.1	0.75	-	11.8	−5.6	0.81

[a]bBS: before bud swelling; aFLU: after final leaf unfolding.

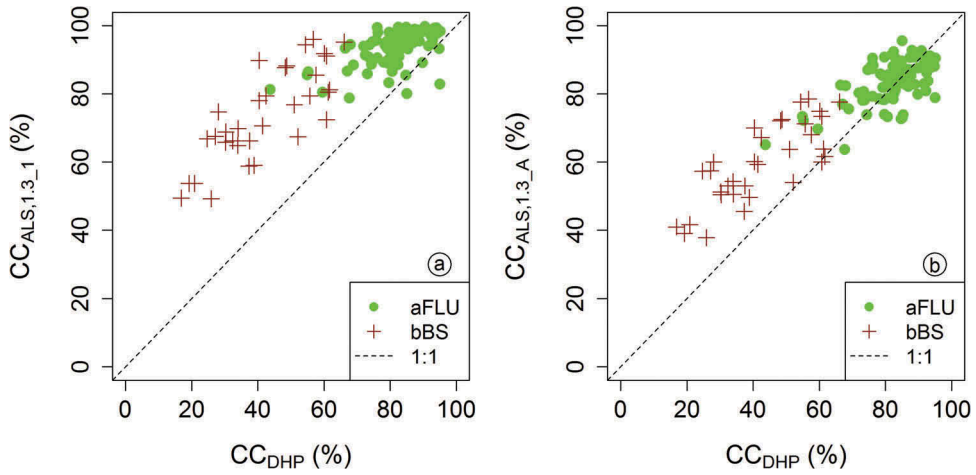

Figure 1. First echoes-based canopy cover (CC) calculated at 1.3-m height break $CC_{ALS,1.3\_1}$ saturates in dense forests in summer (aFLU) (a) compared to all echoes-based $CC_{ALS,1.3\_A}$ (b).

for z instead of the point cloud-based H_{LCB_ALS} improved the correlation of $CC_{ALS,LCB}$ with CC_{DHP} (R^2 = 0.22) when tested for aFLU dataset. We found also that CC_{DHP} was almost always smaller than CC_{ALS} (Table 1, Figure 1). Since the gap fraction estimation from DHP with the LinearRatio (Cescatti, 2007) method that is used in HSP software is an unbiased technique (Lang, Kodar & Arumäe, 2013, Lang et al., 2017), the CC_{ALS} is probably overestimated. However, in our study we did not correct CC_{DHP} for within the crown gap fraction which would increase aFLU CC_{DHP} by a few percentages and thus established a good correlation between the mean $CC_{ALS,1.3\_A}$ and CC_{DHP}.

The pulse splitting within the canopy showed also a difference between aFLU and bBS datasets. The pulses were splitting less (p-value < 0.01) and the share of the first returns increased using aFLU data ($P_{1/A}$ = 0.82) compared to the bBS dataset ($P_{1/A}$ = 0.76). This is also one of the reasons for the systematically overestimated CC_{ALS} for bBS data (Figure 1), since the number of returns from the canopy increased.

The comparison of $CC_{ALS,1.3\_1}$ in the ENFR plots that were scanned twice indicated that at a large VNA, the CC estimates for sample plots may vary substantially when calculated from repeated scans taken from different directions – the maximum differences ranged up to 8%. The VNA correction improved the $CC_{ALS,1.3\_1}$ estimation (Figure 2) precision as appeared from the analysis of overlapping scan swaths. The VNA correction also decreased CC_{ALS} by 13% on average, but the scatter between the repeated measurements remained considerable (Figure 2(b)). The VNA uncorrected dataset (Figure 2(a)) showed a slightly weaker correlation between CC_{ALS_Left} and CC_{ALS_Right} (R^2 = 0.81, $RMSE$ = 4.2%) compared to the VNA corrected dataset (Figure 2(b); R^2 = 0.89; $RMSE$ = 3.8%); however, the change in R^2 was statistically insignificant when tested using Sheskin's (2000) statistical test.

The CC_{ALS} of all ENFR plots was then corrected for the VNA and compared to CC_{DHP} (Figure 3). The scan angle correction decreased the MEE of the relationship between $CC_{ALS,1.3\_1}$ and CC_{DHP} from −12.8 to −4.7; however, the change in R^2 was not significant according to the statistical test (Sheskin, 2000). The scan angle correction caused a systematic underestimation of $CC_{ALS,1.3\_A}$ compared to CC_{DHP} with MEE increasing from −2.8 to 5.3, but the increase in R^2 was again not statistically significant.

The percentage of deciduous tree species in the dominant layer of trees had no correlation with the first echo ratio $P_{1/A}$ (R^2 = 0) using the aFLU dataset. Whereas $P_{1/A}$ had a negative moderate correlation with stand relative density (R^2 = 0.35) and a moderate negative correlation with the ALS-based 80th height percentile (H_{P80}; R^2 = 0.56). The VNA had an influence on $P_{1/A}$. The share of pulses giving only a single echo increased with VNA ≥ 10° and the $P_{1/A}$ at VNA ≥ 16° was 2% larger compared to the near nadir $P_{1/A}$ (p-value < 0.01 based on 379 stands scanned at nadir and 420 stands scanned at VNA>16°).

In contrary to the expected relationship between CC_{ALS} and tree crown-based CC, the concentric ring-based CC_{RCrown} showed no correlation with CC_{DHP} or CC_{ALS}. The neighbourhood corrected CC_{RCrown} showed a weak correlation with CC_{DHP} (R^2 = 0.14) and also with $CC_{ALS,1.3\_A}$ (R^2 = 0.22) and $CC_{ALS,1.3\_1}$ (R^2 = 0.14). Our test with the excluded 2-m-wide buffer from outside the sample plots where the crown model may have lacked the influence of external competition did not show a marked increase in the correlations with other CC estimates. The 2-m buffer zone exclusion increased the average of CC_{RCrown} by 2.7% and increased the $R^2$of the CC_{RCrown} relationship with CC_{DHP} (R^2 = 0.18), $CC_{ALS,1.3\_A}$ (R^2 = 0.24) and $CC_{ALS,1.3\_1}$ (R^2 = 0.16), but statistically the influence

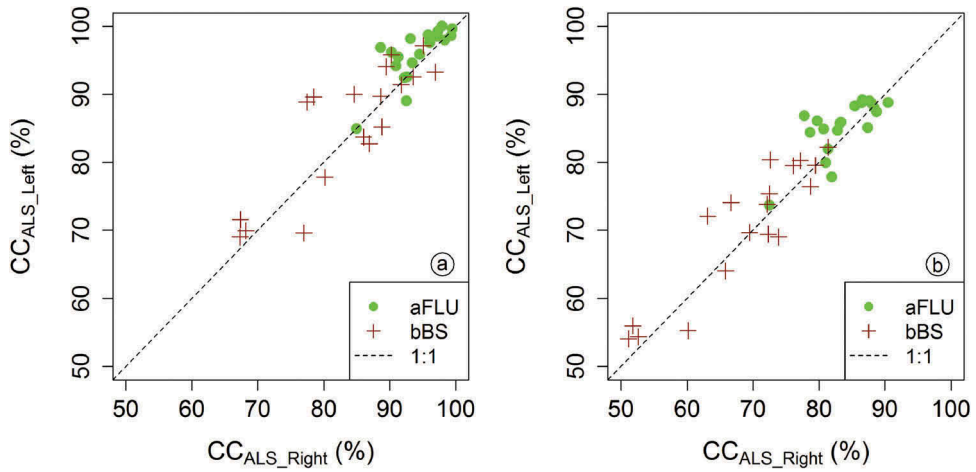

Figure 2. Comparison of CC_{ALS} estimated from the opposite direction flights using the first echoes (a) without VNA correction and (b) using Korhonen and Morsdorf's (2014) VNA correction model.

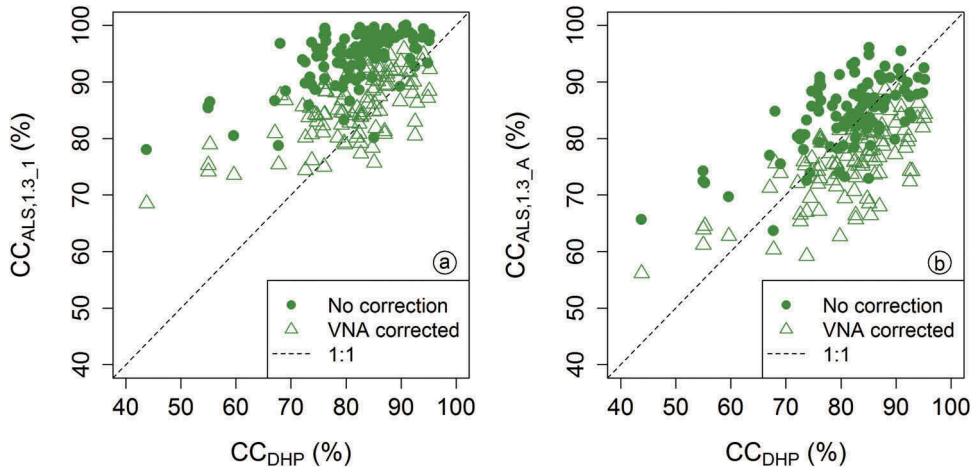

Figure 3. Influence of view nadir angle correction on $CC_{ALS,1.3}$ estimates using the first echoes (a) and using all echoes (b).

was insignificant (p-value > 0.05). The correlation of CC_{RCrown} with CC_{ALS} based on the measured H_{LCB} was weak (R^2 = 0.02), but the mean values of the two CC estimates (67.4% and 69.7%, correspondingly) were closer than CC_{RCrown} and $CC_{ALS,1.3\_A}$ (67.4% and 83.6%, correspondingly).

Discussion

The comparison of CC_{ALS} and CC_{DHP} in the best-case scenario had an *RMSE* of 11.8%, which is comparable to the results of similar studies (Ahmed, Franklin, Wulder, & White, 2015; Smith et al., 2009). The relatively large *RMSE* is most likely the result of measurement errors and comparison of different variables as CC. For example, DHP is measuring light that is penetrating the canopy and the tree crowns are accounted as semi-transparent, as opposed to the CC_{RCrown} which accounts crowns as solid shapes, but ALS-based measurements use the NIR spectral region where also foliage is semi-transparent. Also, the ALS observations are not points, but samples with an area defined usually by the laser beam divergence and flight altitude (Baltsavias, 1999). Sample plot position errors also propagate into CC_{ALS} and decrease the reliability of the CC estimates. Although we found that $CC_{ALS,1.3\_A}$ was usually not substantially influenced by the positioning errors of sample plots, this was probably due to the ENFR plots being well-positioned in homogeneous parts of forest stands. On the other hand, CC_{ALS} calculated for a sample plot using ALS point clouds from different flight paths had an uncertainty of up to 8% in CC units in the forests.

Somewhat surprisingly, there was only a weak correlation between CC_{RCrown} and $CC_{ALS,z}$. This is most likely because CC_{RCrown} and $CC_{ALS,z}$ are different by their definition or is because of the used R_{Crown} models, which were not able to predict accurately tree crown radius in the dense stands. One reason might be also the influence of understory trees, for which there was no data to calculate CC_{RCrown} estimates.

However, there was not much of an improvement in correlation when CC_{ALS} was estimated at measured H_{LCB} threshold to exclude the influence of understory vegetation. Only the mean value of CC_{RCrown} was in a better agreement with $CC_{ALS,LCB}$ compared to $CC_{ALS,1.3}$. The correlation of CC_{RCrown} with CC_{DHP} and $CC_{ALS,LCB}$ did not show a significant improvement after adjusting crown shapes, however, the CC_{RCrown} was estimated according to the competition of neighbouring trees. It is possible that the tree crown shapes vary in nature much more than predicted by the model, and in semi-naturally developed forests, tree stems are not strictly vertical due to competition during their growth. As a result, the CC can be much larger in many plots compared to the estimates based on the crown projections and assumed vertical stems at tree stump locations.

In the dense forests, the CC_{ALS} was estimated using the regular height break z = 1.3 m and saturated using the first or first of many echoes at CC greater than 80%, whereas the CC_{ALS,z_A} did not saturate. There was not much of an influence on CC_{ALS} from the increase in z until 10 m above the ground or until the H_{LCB} level was reached. Raising the threshold higher than 1.3 m did improve the predictive power of the first echoes, but overall, the relationship between CC_{ALS} and CC_{DHP} was still weak and the change in the determination coefficient was statistically insignificant. Using the ALS-based H_{LCB} as a threshold introduces additional errors in CC caused by the errors in H_{LCB_ALS} estimation. On the other hand, the lack of sensitivity of CC_{ALS} to the change in z is probably caused by the upper layer dense canopy in the forests (images can be found in the appendix in Lang et al., 2014), which captures most of the pulse energy and thus relatively fewer echoes from the lower layers down to the ground vegetation are triggered. On the other hand, there is a clear negative correlation between the leaf area index of upper and lower canopy layers in forests (Chianucci, Puletti, Venturi, Cutini, & Chiavetta, 2014; Kodar et al., 2011). In our test, DHPs were taken always at 1.3 m above the ground and a denser forest understory in the case of a smaller CC of the upper layer can explain the weak correlation between the values of CC_{ALS} calculated using H_{LCB} and CC_{DHP}.

In addition to the selection of pulse returns and discrimination threshold for the CC estimation, there are also sampling problems and issues related to the interaction between the lidar pulse and forest canopy. The laser scanners measure at various VNAs and this raises the question of representativity of higher-order echoes in the case of small sample plots in tall forests. With the VNA increase, the second and higher-order returns are displaced horizontally by $h_{diff} \times \tan(\text{VNA})$, where h_{diff} is the vertical distance between the first and subsequent returns of the lidar pulse. For example, at VNA = 25° and h_{diff} = 21 m, the displacement in the horizontal direction is 9.8 m. Therefore when a pulse is sent out at a large VNA, the first echo is triggered from a plot or grid cell location and the following echoes would be received in a shifted location, but their occurrence is still determined by the part of the canopy that triggered the first echo. This makes the CC_{ALS} estimate dependent on the grouping of trees and sensitive to variation in forest height. However, there was a positive correlation between the VNA and canopy $P_{1/A}$ at larger scan angles (VNA>15°) meaning fewer returns per pulse at the view angles. The reasons for this may include the increase in footprint size at larger scanning angles (Heritage & Large, 2009; Korhonen, Korpela, Heiskanen & Maltamo, 2011) and the fact that at large scan angles the probability of seeing crown sides increases and so does the path length through the canopy. The increased path length within the forest canopy causes more scattering which flattens the distribution of the received energy leaving less chance for the scanner internal software to distinguish more than just the first return from emitted pulses.

Additionally to the VNA, the species composition is known to influence the point cloud height distribution and therefore the estimates of CC_{ALS} (Wasser, Day, Chasmer, & Taylor, 2013). The higher reflectance of deciduous broadleaf tree species in NIR should, in theory, result in a greater $P_{1/A}$ as the pulses are being split less due to a stronger signal from the top of the canopy. However, based on the 6185 forest stands, the fraction of broadleaf trees in the upper layer had no influence on $P_{1/A}$, but $P_{1/A}$ was influenced by the structural features of the forest – stand density and height. The correlation between $P_{1/A}$ and forest height is partially explained by the fact that the Leica ALS50-II scanner can register up to four echoes from a single pulse, with a minimum distance of greater than 3.5 m between the echoes. Therefore, the splitting of pulses can only occur in forests where the tree height exceeds the multiple value of the spacing distance. The $P_{1/A}$, and therefore CC_{ALS}, is also influenced by the scanner automatic gain control (AGC) (Vain, Yu, Kaasalainen, & Hyyppa, 2010) which regulates the intensity of the emitted pulses, but the effect was not studied in this research. Similarly to AGC, which regulates the emitted energy, the flight altitude and, in turn, the footprint size has an effect on echo registration (Gaveau & Hill, 2003). The increased pulse splitting found on ENFR plots during bBS compared to aFLU phenophase may also be one reason why all returns-based CC_{ALS} estimates were still systematically greater compared to CC_{DHP} in spring, while there was a good agreement in summer. Similarly to Straatsma and Middelkoop (2006) we found that there were fewer second or higher-order returns per pulse in summer triggered by the

canopy compared to leafless conditions in spring. This is related to the higher NIR reflectance of the foliage compared to leafless branches, which creates a better-defined mode value into the distribution of returned photons. However, CC_{ALS} and CC_{DHP} both showed a consistent increase in CC in accordance with the foliage phenology. The phenology-driven change in CC_{ALS} may be an indicator of the share of deciduous species in the estimation of species composition in forest stands.

To account for the complex influence of the VNA on CC_{ALS} estimates, we applied the VNA correction model published by Korhonen and Morsdorf (2014). In general, there was a small increase in correlation between the CC_{ALS} and CC_{DHP} and a decrease in *RMSE*, but the improvement was statistically insignificant. The VNA correction of $CC_{ALS,1.3\_A}$ resulted in a systematically smaller estimate compared to CC_{DHP} and is therefore not recommended for $CC_{ALS,1.3\_A}$. This indicates that the VNA correction models for ALS-based CC estimates are dependent on the selection of pulse returns, since the model was originally constructed for the first returns of laser pulses. For future studies, a VNA correction model also for all returns-based CC_{ALS} should be developed.

Conclusion

We analysed discrete-return ALS data from dense deciduous broadleaf-dominated mixed forests for CC estimation using references obtained from tree crown models and DHP. The uncertainties in the ALS-based CC estimates due to the errors in sample plot location and sampling of point clouds from different scans at large VNAs are roughly in the same range and reach up to 8–10% in CC units in the stands. Correction of VNA effects systematically decreased CC estimates, but did not decrease variability and there was no improvement in the correlation with CC estimated from DHPs. A VNA effect correction model developed for the first returns yields biased CC values when applied to all returns-based CC estimates. There is not much of an influence on ALS-based CC estimates when selecting a threshold height from the range between 1.3 m above the ground and the level of the live crown base in the dense forests.

There was a good agreement between the CC estimated from ALS data and DHPs, while both estimates had only a weak correlation with the CC based on crown radius models. The weak correlation was probably related to the different meaning of the variables and failure of crown models to account for single tree crown plasticity in the dense forests. The increase in foliage density decreases the number of returns per pulse triggered from the forest canopy. This effect may be important for ALS-based defoliation estimates which will be thus less sensitive to an actual decrease in foliage density. In general, the number of returns per pulse in the aFLU phenophase ALS data was not dependent on the proportion of broadleaf trees but only on forest height and stand relative density. Finally, for the estimation of CC using ALS data in the dense forests, we recommend using the first returns and VNA effect correction or all returns without the correction.

Acknowledgments

The authors would like to thank the Estonian Land Board for the airborne lidar data. Data acquisition was financed by the Estonian State Forest Management Centre. Ave Kodar helped during field measurements. Data analysis was supported by the Ministry of Education and Research grant IUT21-4. The Estonian Network of Forest Research Plots was supported by the Estonian State Forest Management Centre and the Estonian Environmental Investment Centre. The authors are also thankful for the helpful comments from the anonymous reviewers.

Disclosure statement

No potential conflict of interest was reported by the authors.

References

Ahmed, O.S., Franklin, S.E., Wulder, M.A., & White, J.C. (2015). Characterizing stand-level forest canopy cover and height using Landsat time series, samples of airborne LiDAR, and the random forest algorithm. *ISPRS Journal of Photogrammetry and Remote Sensing*, *101*, 89–101. doi:10.1016/j.isprsjprs.2014.11.007

Andersen, H.-E., McGaughey, R.J., & Reutebuch, S.E. (2005). Estimating forest canopy fuel parameters using LIDAR data. *Remote Sensing of Environment*, *94*, 441–449. doi:10.1016/j.rse.2004.10.013

Arumäe, T., & Lang, M. (2013). A simple model to estimate forest canopy base height from airborne lidar data. *Forestry Studies*, *58*, 46–56. doi:10.2478/fsmu-2013-0005

Arumäe, T., & Lang, M. (2016a). A validation of coarse scale global vegetation height map for biomass estimation in hemiboreal forests in Estonia. *Baltic Forestry*, *22* (2), 275–282. Retrieved from https://www.balticforestry.mi.lt/bf/index.php?option=com_content&view=article&catid=14&id=455

Arumäe, T., & Lang, M. (2016b). ALS-based wood volume models of forest stands and comparison with forest inventory data. *Foresty Studies*, *64*, 5–16. doi:10.1515/fsmu-2016-0001

Baltsavias, E.P. (1999). Airborne laser scanning: Basic relations and formulas. *ISPRS Journal of Photogrammetry & Remote Sensing*, *54*, 199–214. doi:10.1016/S0924-2716(99)00015-5

Bouvier, M., Durrieu, S., Fournier, R.A., & Renaud, J.-P. (2015). Generalizing predictive models of forest inventory attributes using an area-based approach with airborne LiDAR data. *Remote Sensing of Environment*, *156*, 322–334. doi:10.1016/j.rse.2014.10.004

Bright, B.C., Hicke, J.A., & Hudak, A.T. (2012). Estimating aboveground carbon stocks of a forest affected by mountain pine beetle in Idaho using lidar and multispectral imagery. *Remote Sensing of Environment*, *124*, 270–281. doi:10.1016/j.rse.2012.05.016

Cescatti, A. (2007). Indirect estimates of canopy gap fraction based on the linear conversion of hemispherical photographs: Methodology and comparison with standard thresholding techniques. *Agricultural and Forest Meteorology*, *143*, 1–12. doi:10.1016/j.agrformet.2006.04.009

Chianucci, F., Puletti, N., Venturi, E., Cutini, A., & Chiavetta, U. (2014). Photographic assessment of overstory and understory leaf area index in beech forests under different management regimes in Central Italy. *Forestry Studies*, *61*, 27–34. doi:10.2478/fsmu-2014-0008

Davies, O., & Pommerening, A. (2008). The contribution of structural indices to the modelling of Sitka spruce (*Picea sitchensis*) and birch (*Betula* spp.) crowns. *Forest Ecology and Management*, *256*, 68–77. doi:10.1016/j.foreco.2008.03.052

Duncanson, L.I., Cook, B.D., Hurtt, G.C., & Dubayah, R.O. (2014). An efficient, multi-layered crown delineation algorithm for mapping individual tree structure across multiple ecosystems. *Remote Sensing of Environment*, *154*, 378–386. doi:10.1016/j.rse.2013.07.044

Ferraz, A., Mallet, C., Jacquemoud, S., Gonçalves, G.R., Tomé, M., Soares, P., … Bretar, F. (2015). Canopy density model: A new ALS-derived product to generate multilayer crown cover maps. *IEEE Transactions on Geoscience and Remote Sensing*, *53*, 6776–6790. doi:10.1109/TGRS.2015.2448056

Ferraz, A., Saatchi, S., Mallet, C., Jacquemoud, S., Gonçalves, G., Silva, C.A., … Pereira, L. (2016). Airborne lidar estimation of aboveground forest biomass in the absence of field inventory. *Remote Sensing*, *8*(8), 1–18. doi:10.3390/rs8080653

Ferraz, A., Saatchi, S., Mallet, C., & Meyer, V. (2016). Lidar detection of individual tree size in tropical forests. *Remote Sensing of Environment*, *183*, 318–333. doi:10.1016/j.rse.2016.05.028

Gaveau, D.L.A., & Hill, R.A. (2003). Quantifying canopy height underestimation by laser pulse penetration in small-footprint airborne laser scanning data. *Canadian Journal of Remote Sensing*, *29*, 650–657. doi:10.5589/m03-023

Guerra-Hernández, J., Görgens, E.B., García-Gutiérrez, J., Rodriguez, L.C.E., Tomé, M., & González-Ferreiro, E. (2016). Comparison of ALS based models for estimating aboveground biomass in three types of Mediterranean forest. *European Journal of Remote Sensing*, *49*, 185–204. doi:10.5721/EuJRS20164911

Heritage, G.L., & Large, A.R.G. (2009). Principles of 3D laser scanning. In G.L. Heritage & A.R.G. Large (Eds.), *Laser scanning for the environmental sciences* (pp. 21–34). Chichester: John Wiley & Sons.

Jakobsons, A. (1970). Sambandet mellan trädkronans diameter och andra trädfaktorer, främst brösthöjdsdiametern. [The correlation between the diameter of tree crown and ohter tree factors – Mainly the breastheight diameter]. *Research Notes*, *14*, 75. In Swedish with an English summary.

Jennings, S.B., Brown, N.D., & Sheil, D. (1999). Assessing forest canopies and understorey illumination: Canopy closure, canopy cover and other measures. *Forestry*, *72*, 59–74. doi:10.1093/forestry/72.1.59

Jonckheere, I., Nackaerts, K., Muys, B., & Coppin, P. (2005). Assessment of automatic gap fraction estimation of forests from digital hemispherical photography. *Agricultural and Forest Meteorology*, *132*, 96–114. doi:10.1016/j.agrformet.2005.06.003

Kandare, K., Ørka, H.O., Dalponte, M., Næsset, E., & Gobakken, T. (2017). Individual tree crown approach for predicting site index in boreal forests using airborne laser scanning and hyperspectral data. *International Journal of Applied Earth Observation and Geoinformation*, *60*, 72–82. doi:10.1016/j.jag.2017.04.008

Keränen, J., Maltamo, M., & Packalen, P. (2016). Effect of flying altitude, scanning angle and scanning mode on the accuracy of ALS based forest inventory. *International Journal of Applied Earth Observation and Geoinformation*, *52*, 349–360. doi:10.1016/j.jag.2016.07.005

Kiviste, A., Hordo, M., Kangur, A., Kardakov, A., Laarmann, D., Lilleleht, A., … Korjus, H. (2015). Monitoring and modelling of forest ecosystems: The Estonian Network of Forest Research Plots. *Forestry Studies*, *62*, 26–38. doi:10.1515/fsmu-2015-0003

Kodar, A., Lang, M., Arumäe, T., Eenmäe, A., Pisek, J., & Nilson, T. (2011). Leaf area index mapping with airborne lidar, satellite images and ground measurements in Järvselja VALERI test site. *Forestry Studies*, *55*, 11–32. doi:10.2478/v10132-011-0099-1

Korhonen, L., Korhonen, K.T., Rautiainen, M., & Stenberg, P. (2006). Estimation of forest canopy cover: A comparison of field measurement techniques. *Silva Fennica*, *40*, 577–588. doi:10.14214/sf.315

Korhonen, L., Korpela, I., Heiskanen, J., & Maltamo, M. (2011). Airborne discrete-return LIDAR data in the estimation of vertical canopy cover, angular canopy closure and leaf area index. *Remote Sensing of Environment*, *115*, 1065–1080. doi:10.1016/j.rse.2010.12.011

Korhonen, L., & Morsdorf, F. (2014). Estimation of canopy cover, gap fraction and leaf area index with airborne laser scanning. In *Forestry applications of airborne laser scanning: Concepts and case studies* (pp. 397–417). Dordrecht: Springer. doi:10.1007/978-94-017-8663-8

Kuusk, A., Lang, M., & Kuusk, J. (2013). Database of optical and structural data for the validation of forest radiative transfer models. In *Light scattering reviews* (Vol. *7*, pp. 109–148). Berlin, Heidelberg: Springer. doi:10.1007/978-3-642-21907-8

Kuusk, A., & Nilson, T. (2000). A directional multispectral forest reflectance model. *Remote Sensing of Environment*, *72*, 244–252. doi:10.1016/S0034-4257(99)00111-X

Lang, M. (2010). Estimation of crown and canopy cover from airborne lidar data. *Forestry Studies*, *52*, 5–17. doi:10.2478/v10132-011-0079-5

Lang, M., Arumäe, T., & Anniste, J. (2012). Estimation of main forest inventory variables from spectral and airborne lidar data in Aegviidu test site, Estonia. *Forestry Studies*, *56*, 27–41. doi:10.2478/v10132-012-0003-7

Lang, M., Arumäe, T., Lükk, T., & Sims, A. (2014). Estimation of standing wood volume and species composition in managed nemoral multi-layer mixed forests by using nearest neighbour classifier, multispectral satellite images and airborne lidar data. *Forestry Studies*, *61*, 47–68. doi:10.2478/fsmu-2014-0010

Lang, M., Kodar, A., & Arumäe, T. (2013). Restoration of above canopy reference hemispherical image from below

canopy measurements for plant area index estimation in forests. *Forestry Studies*, *59*, 13–27. doi:10.2478/fsmu-2013-0008

Lang, M., & Kurvits, V. (2007). Restoration of tree crown shape for canopy cover estimation. *Forestry Studies*, *46*, 23–34. doi:10.2478/v10132-011-0079-5

Lang, M., Nilson, T., Kuusk, A., Kiviste, A., & Hordo, M. (2007). The performance of foliage mass and crown radius models in forming the input of a forest reflectance model: A test on forest growth sample plots and Landsat 7 ETM+ images. *Remote Sensing of Environment*, *110*, 445–457. doi:10.1016/j.rse.2006.11.030

Lang, M., Nilson, T., Kuusk, A., Pisek, J., Korhonen, L., & Uri, V. (2017). Digital photography for tracking the phenology of an evergreen conifer stand. *Agricultural and Forest Meteorology*, *246*, 15–21. In press. doi:10.1016/j.agrformet.2017.05.021

Leica. (2007). Leica ALS50-II airborne laser scanner product specifications. Retrieved from http://www.nts-info.com/inventory/images/ALS50-II.Ref.703.pdf

Lilleleht, A., Sims, A., & Pommerening, A. (2014). Spatial forest structure reconstruction as a strategy for mitigating edge-bias in circular monitoring plots. *Forest Ecology and Management*, *316*, 47–53. doi:10.1016/j.foreco.2013.08.039

Lõhmus, E. (2004). *Estonian site types* (pp. 80). Tartu: Eesti Loodusfoto.

McGaughey, R.J. (2014). *FUSION/LDV: Software for LIDAR data analysis and visualization. March 2014 – FUSION, version 3.42*. United States Department of Agriculture Forest Service Pacific Northwest Research Station. http://forsys.cfr.washington.edu/fusion/FUSION_manual.pdf

Moeser, D., Roubinek, J., Schleppi, P., Morsdorf, F., & Jonas, T. (2014). Canopy closure, LAI and radiation transfer from airborne LiDAR synthetic images. *Agricultural and Forest Meteorology*, *197*, 158–168. doi:10.1016/j.agrformet.2014.06.008

Mongus, D., & Žalik, B. (2015). An efficient approach to 3D single tree-crown delineation in LiDAR data. *ISPRS Journal of Photogrammetry and Remote Sensing*, *108*, 219–233. doi:10.1016/j.isprsjprs.2015.08.004

Müller, J., & Vierling, K. (2014). *Assessing biodiversity by airborne laser scanning* (pp. 357–374). Dordrecht: Springer. doi:10.1007/978-94-017-8663-8

Næsset, E. (1997a). Determination of mean tree height of forest stands using airborne laser scanner data. *ISPRS Journal of Photogrammetry & Remote Sensing*, *52*, 49–56. doi:10.1016/S0924-2716(97)83000-6

Næsset, E. (1997b). Estimating timber volume of forest stands using airborne laser scanner data. *Remote Sensing of Environment*, *61*, 246–253. doi:10.1016/S0034-4257(97)00041-2

Nilson, T., & Kuusk, A. (2004). Improved algorithm for estimating canopy indices from gap fraction data in forest canopies. *Agricultural and Forest Meteorology*, *124*, 157–169. doi:10.1016/j.agrformet.2004.01.008

Nilson, T., Lang, M., Kuusk, A., Anniste, J., & Lükk, T. (2000). Forest reflectance model as an interface between satellite images and forestry databases. In *Remote sensing and forest monitoring. IUFRO conference* (pp. 462–476). Luxembourg: Office for Official Publications of the European Communities.

Patenaude, G., Hill, R.A., Milne, R., Gaveau, D.L.A., Briggs, B.B.J., & Dawson, T.P. (2004). Quantifying forest above ground carbon content using LiDAR remote sensing. *Remote Sensing of Environment*, *93*, 368–380. doi:10.1016/j.rse.2004.07.016

Popescu, S.C., Zhao, K., Neuenschwander, A., & Lin, C. (2011). Satellite lidar vs. small footprint airborne lidar: Comparing the accuracy of aboveground biomass estimates and forest structure metrics at footprint level. *Remote Sensing of Environment*, *115*, 2786–2797. doi:10.1016/j.rse.2011.01.026

Purves, D.W., Lichstein, J.W., & Pacala, S.W. (2007). Crown plasticity and competition for canopy space: A new spatially implicit model parameterized for 250 North American tree species. *PLOS One*, *2*(9), 1–11. doi:10.1371/journal.pone.0000870

Rautiainen, M., Stenberg, P., & Nilson, T. (2005). Estimating canopy cover in Scots pine stands. *Silva Fennica*, *39*(1), 137–142. doi:10.14214/sf.402

Sheskin, D.J. (2000). *Parametric and nonparametric statistical procedures* (2nd ed., pp. 779–783). Boca Raton: Chapman & Hall/CRC.

Smith, A.M.S., Anderson, J., & Fladeland, M. (2008). Forest canopy structural properties. In *Field measurements for forest carbon monitoring* (pp. 179–196). New York, NY: Springer. doi:10.1007/978-1-4020-8506-2

Smith, A.M.S., Falkowski, M.J., Hudak, A.T., Evans, J.S., Robinson, A.P., & Steele, C.M. (2009). A cross-comparison of field, spectral, and lidar estimates of forest canopy cover. *Canadian Journal of Remote Sensing*, *35*, 447–459. doi:10.5589/m09-038

Solberg, S., Brunner, A., Hanssen, K.H., Lange, H., Næsset, E., Rautiainen, M., & Stenberg, P. (2009). Mapping LAI in a Norway spruce forest using airborne laser scanning. *Remote Sensing of Environment*, *113*, 2317–2327. doi:10.1016/j.rse.2009.06.010

Spurr, S.H. (1948). *Aerial photographs in forestry* (pp. 340). New York, NY: Ronald Press.

Straatsma, M.W., & Middelkoop, H. (2006). Airborne laser scanning as a tool for lowland floodplain vegetation monitoring. *Hydrobiologia*, *565*, 87–103. doi:10.1007/s10750-005-1907-5

Vain, A., Yu, X., Kaasalainen, S., & Hyyppä, J. (2010). Correcting airborne laser scanning intensity data for automatic gain control effect. *IEEE Geoscience and Remote Sensing Letters*, *7*, 511–514. doi:10.1109/LGRS.2010.2040578

Vastaranta, M., Holopainen, M., Yu, X., Hyyppä, J., Hyyppä, H., & Viitala, R. (2011). Predicting stand-thinning maturity from airborne laser scanning data. *Scandinavian Journal of Forest Research*, *26*, 187–196. doi:10.1080/02827581.2010.547870

Wasser, L., Day, R., Chasmer, L., & Taylor, A. (2013). Influence of vegetation structure on lidar-derived canopy height and fractional cover in forested riparian buffers during leaf-off and leaf-on conditions. *PLOS One*, *8*, 1–13. doi:10.1371/journal.pone.0054776